ISSN 1023-1935, Russian Journal of Electrochemistry, 2020, Vol. 56, No. 8, pp. 669–679. © Pleiades Publishing, Ltd., 2020.
Published in Russian in Elektrokhimiya, 2020, Vol. 56, No. 8, pp. 737–748.

Electrochemical Investigation of Lithium Ion Battery Including $LiCo_{0.8}Ni_{0.2}O_2$, Li_2MnO_3, $LiNiO_2$ Cathode Materials

M. Monajjemi[a, b, *], F. Mollaamin[b], P. T. Thu[b], M. Otadi[a], A. Alihosseini[a], D. T. M. Dung[b], and D. M. Chien[b]

[a] *Department of Chemical Engineering, Central Tehran Branch, Islamic Azad University, Tehran, Iran*
[b] *Institute for Nanotechnology (INT), Vietnam National University-Ho Chi Minh City (VNUHCM), Ho Chi Minh City, Vietnam*
**e-mail: Maj.monajjemi@iauctb.ac.ir*

Received November 10, 2018; revised May 27, 2019; accepted July 29, 2019

Abstract—$(1 - n - m)LiCo_{0.8}Ni_{0.2}O_2$ system was synthesized using the sol–gel method. Stoichiometric weights of the $LiNO_3$, $Mn(Ac)_2 \cdot 4H_2O$, $Co(Ac)_2 \cdot 4H_2O$, $Ni(NO_3)_2 \cdot 6H_2O$ for preparing of 28 samples have been used as starting materials of lithium, magnesium, cobalt and nickel, in 28 samples of $(1 - n - m)LiCo_{0.8}Ni_{0.2}O_2$, respectively. We exhibited "$Li_{1.333}Ni_{0.4}Co_{0.267}Mn_{0.333}O_2$" is the best composition for cathode material among those compositions. Obviously, the used weight of cobalt in this sample is lower compared with $LiCoO_2$ that is an advantage in view point of cost and toxic problem. Charge–discharge characteristics of the mentioned cathode materials were investigated by performing cycle tests in the range of 2.2–4.5 V. Our results confirmed, although these kind systems can help for removing the disadvantage of cobalt which mainly is its cost and toxic, the performance of these kind systems are similar to $LiCoO_2$ cathode material.

Keywords: lithium ion battery, sol–gel method, cathode material
DOI: 10.1134/S1023193520030076

INTRODUCTION

Transition elements of cathode materials including nickel, manganese, cobalt (NMC), are especial metals for lithium ion batteries (LIBs) due to their potentials for operating in high voltages and large energy storing in a small space. Although the Ni in NMC gives a high capacity for storing energies, it is also passive and unstable, with a propensity towards destructive reactions with the electrolyte. As it can be seen in Table 1 there are both advantages and disadvantages factors for NMC of LIBs [1–5]. A major disadvantage of cobalt is its cost and toxic and typically it is around two times more costly to manufacture than nickel. This is one important factor when considering its use in mass produced consumer items which any extra cost is a basic issue. Safety factor is also a matter of crucial importance to the lithium ion batteries which this problem appears in big size batteries as compared to the small size batteries i.e. batteries for electric vehicle would have more risk of catching fire as compared to batteries for cell phones. When mixed solid solution is used as cathode material, the explosion of batteries can be control, especially with doping of other elements such as Mg and Al. Moreover $LiNi_xCo_yMn_zO_2$ are environment friendly as compared to isolated cathode such as $LiCoO_2$ [4, 5].

The purpose of this study is to find a ternary solid solution of Li-based cathode material in NMC that is advantageous replacement for $LiCoO_2$ which is expensive and toxic. Therefore a combination of ternary composition diagram including $(1 - x - y)LiNi_{0.7}Co_{0.3}O_2$, xLi_2MnO_3 and $yLiCoO_2$ have been considered. NMC LIBs were the most interest among the scientist to replace with $LiCoO_2$ which firstly reported by Rossen et al. in 1992 [6] for composition of $LiNi_{0.5}Mn_{0.5}O_2$.

Similar the work of Rossen [6], a study was reported in 1998 by Saphr et al. [7] in view point of electrochemical behavior which indicate Ni as an active ion and Mn were present in "+2" and "+4" oxidation rather the "+3". They exhibited in temperature of 750°C there are a large falling capacity after 25 cycle from 150 to 125 mA h/g after 25 cycles and to 75 mA h/g after 50 cycles. Nickel, which forms between +2 and +4 valences positions is active material in this cathode composition, meanwhile manganese is +4, which remain without Jahn–Teller distortion with the +3 valance (Mn^{3+}). Makimura and coworkers [8] presented an initial discharging around 150.5 mA h/g for 30 cycles at 4.35 V and again in 2003 [9] their results exhibited 200 mA h/g of rechargeable capacity of $LiNi_{1/2}Mn_{1/2}O_2$ among the voltages of 2.5–4.5 V after 30 cycles [9].

Table 1. Characteristics of commercial Li-ion battery cathode materials [5]

Material	Potential versus Li/Li^+	Capacity, mA h g^{-1}	Energy, W h kg^{-1}	Advantage	Disadvantage
$LiCoO_2$	3.9	140	546	Low	High
NCA (Nickel, Cobalt, Aluminum)	3.8	180–200	680–760	Slow reaction with electrolyte High capacity, high voltage Excellent high rate performance	High cost of Ni and Co
NMC (Nickel, Manganese, Cobalt)	3.8	160–170	610–650	High capacity, high operating voltage Slow reaction with electrolyte Moderate safety (oxygen release)	High cost of Ni and Co
$LiMn_2O_4$ (LMO)	4.1	100–120	410–492	Low cost, moderate safety (oxygen release), excellent high rate performance, high operating voltage	Low capacity, affecting cycle life
$LiFePO_4$ (LFP)	3.45	150–170	518–587	Low cost, excellent high rate performance, slow reaction with electrolyte, excellent safety (oxygen release)	Low voltage Low capacity

Obviously, mixing proper mole fractions of various transition elements [8, 9] to get the advantageous efficiency of each led to the discovery of these kind materials. Therefore these materials are derived from $Li(Ni_{(1-x-y)}Mn_xCo_y)O_2$ categorize that were first published in 1999 and 2000 by Liu and Yoshio, respectively [10, 11]. They exhibited that the enhancement of cobalt would stabilize the composition blocks the Ni from entering the lithium layers. Meanwhile, nickel and manganese would provide the structural stabilities and high capacities respectively. As too much of cobalt causes decreasing capacities and large amount of nickel and manganese making problems in cation mixing and spinel structures, therefore mixing of these elements must be optimized with suitable mole fraction.

Makimura and coworkers in 2001 synthesize the layered compound of $LiNi_{1/3}Mn_{1/3}Co_{1/3}O_2$ [12] and exhibited that this cathode has about 205 mA h/g reversible discharge capacity in the range of 2.6–4.5 V including large rate capabilities and thermal stabilities.

For appropriate stoichiometry of $Li(Ni_xCo_{(1-2x)}Mn_x)O_2$, $x = 1/3$, the medium oxidation numbers must be +3 such as Mn^{4+}, Co^{3+}, and Ni^{2+}, with electrochemical flow in the ranges between 2.5 up to 4.4 volte versus lithium ions (through two electron transfer reaction between Co^{3+}/Co^{4+} and Ni^{2+}/Ni^{4+}) [13]. In addition concerning of further electrochemical phenomenon some more studies of $LiNi_{0.4}Mn_{0.4}Co_{0.2}O_2$ [14], $Li(Ni_{0.8}Co_{0.2})O_2$ and $LiNi_{0.8}Co_{0.15}Al_{0.05}O_2$ cathodes [15] have been shown. Although the rate capability of this material is smaller than that of $LiCoO_2$, thermal stabilities are much better.

In this work we focused on various composition of binary and ternary solid solutions containing Li_2MnO_3, $LiNiO_2$ and $(1-n-m)LiCo_{0.8}Ni_{0.2}O_2$ (Scheme 1). Currently, Li_2MnO_3 has been distinguished for its suitable capacity, better safety, without toxic and inexpensive than $LiCoO_2$ [16].

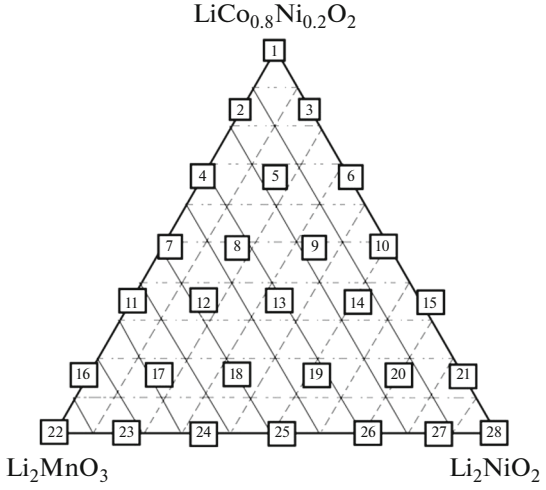

Scheme 1. Binary and ternary diagram of $(1-n-m)LiCo_{0.8}Ni_{0.2}O_2$, $mL_{i2}MnO_3$ and $nLiNiO_2$ compositions.

Table 2. 28 different composition points according to using the lever rule, stoichiometric weights and mole-fractions of the triangle diagram

Sample	Composition	Sample	Composition
1	$LiNi_{0.2}Co_{0.8}O_2$	15	$LiNi_{0.733}Co_{0.267}O_2$
2	$Li_{1.167}Ni_{0.167}Co_{0.666}Mn_{0.167}O_2$	16	$Li_{1.835}Ni_{0.033}Co_{0.132}Mn_{0.835}O_2$
3	$LiNi_{0.334}Co_{0.666}O_2$	17	$Li_{1.667}Ni_{0.2}Co_{0.132}Mn_{0.667}O_2$
4	$Li_{1.333}Ni_{0.133}Co_{0.533}Mn_{0.333}O_2$	18	$Li_{1.5}Ni_{0.368}Co_{0.132}Mn_{0.5}O_2$
5	$Li_{1.167}Ni_{0.3}Co_{0.533}Mn_{0.167}O_2$	19	$Li_{1.333}Ni_{0.535}Co_{0.132}Mn_{0.333}O_2$
6	$LiNi_{0.467}Co_{0.533}O_2$	20	$Li_{1.167}Ni_{0.7}Co_{0.132}Mn_{0.167}O_2$
7	$Li_{1.5}Ni_{0.1}Co_{0.4}Mn_{0.5}O_2$	21	$LiNi_{0.868}Co_{0.132}O_2$
8	$Li_{1.333}Ni_{0.267}Co_{0.4}Mn_{0.333}O_2$	22	Li_2MnO_3
9	$Li_{1.167}Ni_{0.433}Co_{0.4}Mn_{0.167}O_2$	23	$Li_{1.833}Ni_{0.167}Mn_{0.833}O_2$
10	$Li\ Ni_{0.6}Co_{0.4}O_2$	24	$Li_{1.667}Ni_{0.333}Mn_{0.667}O_2$
11	$Li_{1.667}Ni_{0.o66}Co_{0.267}Mn_{0.667}O_2$	25	$Li_{1.5}Ni_{0.5}Mn_{0.5}O_2$
12	$Li_{1.5}Ni_{0.233}Co_{0.267}Mn_{0.5}O_2$	26	$Li_{1.333}Ni_{0.667}Mn_{0.333}O_2$
13	$Li_{1.333}Ni_{0.4}Co_{0.267}Mn_{0.333}O_2$	27	$Li_{1.167}Ni_{0.833}Mn_{0.167}O_2$
14	$Li_{1.167}Ni_{0.567}Co_{0.267}Mn_{0.167}O_2$	28	$LiNiO_2$

Li_2MnO_3 which can be demonstrated as $Li(Li_{1/3}Mn_{2/3})O_2$ has a similar structure as $LiCoO_2$, but there is super-lattice ordering of Li^+ and Mn^{4+} in transition metal layers. Li_2MnO_3 has a layered rock like shape which is consist of lithium and manganese ions in alternating (1 : 2 ratio respectively) positions and the layers are separated via a cubic oxygen layer.

As manganese is present in +4 oxidation number, it is impossible to be further oxidization in low voltages therefore Li_2MnO_3 might be electrochemically inactive, whereas this material in higher voltages i.e. >4.4 V will extract the lithium ions (in the form of Li_2O) through behind of MnO_2 layers. Meanwhile, the mentioned mechanism is unilateral and not reversible therefore only one Li^+ ion can return during discharging towards $LiMnO_2$ structure which is an active material. The extra lithium atom which refracts within charging attaches to the higher capacities. Using of cathodes with Li_2MnO_3 is important due to simplify the intercalation mechanism and also providing structural stabilities during this intercalation [17].

Solid solutions were basically elected in terms of obtaining a cathode composition with superior efficiency of cyclability, capacity and structural stabilities also with costs low. By a few works the solid solutions have been applied as cathode material including both binary and ternary systems [18, 19]. Solid solutions containing Li_2MnO_3 were found suitable for two major sake, one the extraction of two Li^+ ions at voltages >4.4 V which gives the extra amount of initial charge capacities and second the MnO_2 ingredient that on removal of lithium gives well structural stability in that composition.

It is notable that the initial crystal structures of the cathode material not only specifies the initial characteristic capacity, but also imply to the stability. The consistency of de-lithiated cathode materials is substantial for any increasing of the cycle life. During the lithium-ion extracting, nickel and cobalt will be oxidized from +3 to +4 valance positions, so the crystal cell volume will be change. Therefore in the system of $(1 - n - m)LiCo_{0.8}Ni_{0.2}O_2$ composite (Table 2), the high nickel content usually gives higher initial specific

capacities while cobalt improve the structural stabilities and life cycle. Not only, Ni improves the capacity retention [20] well but also promotes the diffusion of Li^+ in $(1 - n - m)LiCo_{0.8}Ni_{0.2}O_2$, mLi_2MnO_3, $nLiNiO_2$ composition. Moreover, it represses the phase transitions that usually occur in $LiNiO_2$ during cycling and improves the charge–discharge reversibility of related composition.

EXPERIMENTAL SECTION

The composites were synthesized using the sol–gel method due to simple chemical reaction with a low temperature and a high degree of homogeneity. Stoichiometric weights of the $LiNO_3$, $Mn(Ac)_2 \cdot 4H_2O$, $Co(Ac)_2 \cdot 4H_2O$, $Ni(NO_3)_2 \cdot 6H_2O$ as starting materials of lithium, magnesium, manganese, cobalt and nickel, in 28 samples of $(1 - n - m)LiCo_{0.8}Ni_{0.2}O_2$, respectively. These mixtures were first dissolved in 50 mL of DI H_2O and then equivalence-molar weights of citric acid were added (the amount of citric acid was equal to the total molar of Co, Ni, and Mn). The whole mixtures were heated through water bath at 100°C and during the heating process, a clear, pink solution without any precipitation formed. At last, the clear solution was slowly dried and turned into gel. This solution was continuously stirred for about 20 min for the formation of a homogeneous mixture of gel and then is kept under a hot-plate for 12–14 h around 100°C so that all the distilled water gets evaporated. Usually, acetate requires two heating temperatures (low and high) for the formation of a correct phase. The beaker containing the gel is then kept in a furnace and is heated to 400°C for 4–6 h. The first heating is at a low temperature. Basically, what happens during this stage is that all the acetates present would get burned off, but the desired phase is not formed. The heat-treated products were ground in an agate mortar to obtain powders and then the powder was calcined at 750–800°C for 8–10 h. It is notable that the 2nd heating is done at so higher temperatures because of the wide range of materials present in the composition and also more importantly to ensure the formation of a proper phase for the crystalline structure then the material collected from the furnace is stored at a dry place until it is made into a cathode. For fabrication of cathodes, the prepared products were fist mixed with acetylene black and poly-vinylidene fluoride in N-methyl-pyrrolidone (NMP).

Acetylene black is added to improve the electrical conductivities and NMP is added mainly to hold the mixture together. For the systems a Glove-Box model of kk-011AD (Serial no. kk-1760) has been used (Scheme 2).

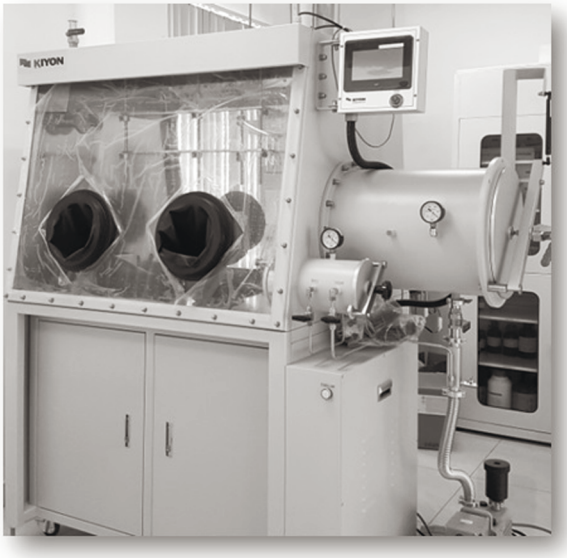

Scheme 2. The glove box model kk-011AD in Institute for Nanotechnology, Vietnam National University—Ho Chi Minh City, Vietnam.

The electrochemical tests were done using CR2032 coin-type cells, which consist of the cathode, lithium foil as the anode. The cells were charged and discharged at room temperature in the voltage range of 2.4–4.6 V (versus Li/Li^+). Cyclic voltammograms of $Li_{1.333}Ni_{0.4}Co_{0.267}Mn_{0.333}O_2$ were obtained by IM6 in the voltage range 2.4–4.6 V at a scanning rate of 0.1 mV s^{-1}. The reference and counter electrodes were fabricated from lithium metal.

Cathode Preparation

The phase identity and crystal structure of the materials were investigated by measuring X-ray diffraction (Bruker, Germany) and the surface morphology was observed via a scanning electron microscopy (SEM) Schemes 3 and 4. These kind tests have been performed for verifying the composition for analyzing the morphology of those synthesized samples. In Schemes 3 and 4, SEM morphology has been presented in a suitable phase (between 1–10 microns for particle sizes) which is important for the increasing the performance of the battery. The samples were made for cathode preparation, which is commonly used in lab testing. It was verified that none of the electrodes showed visible imperfections such as cracks present on the surface of the electrode and that they were all of uniform thickness and also the synthesis condition for all the samples were in the same condition. Based on our previous works, the data has been analyzed by solvent and Nano molecular scales [21–25].

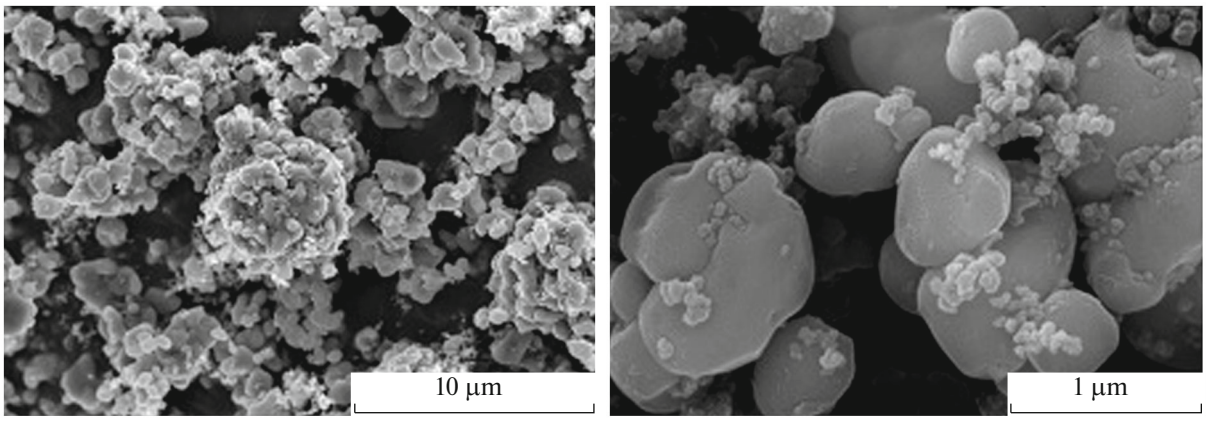

Scheme 3. Scanning electron micrograph obtained for $LiCo_{0.8}Ni_{0.2}O_2$.

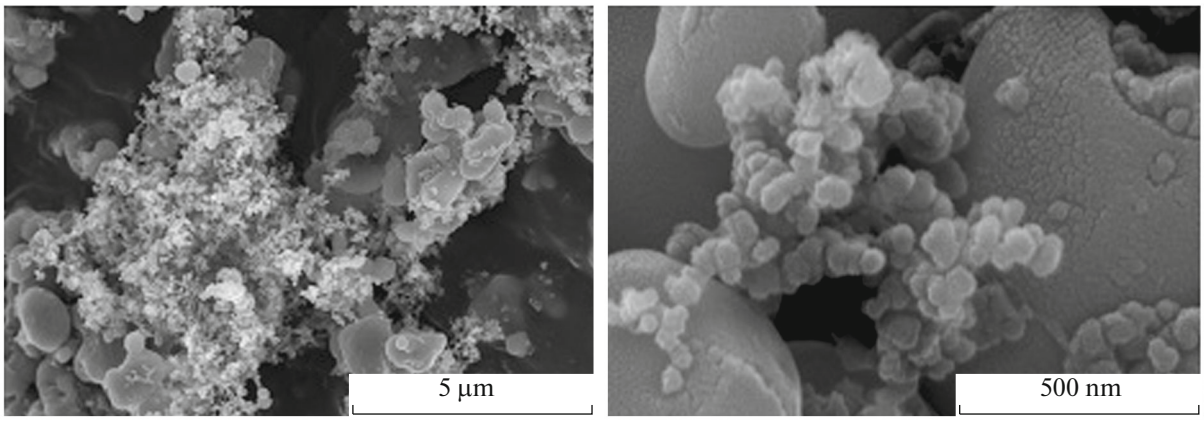

Scheme 4. Scanning electron micrograph obtained for Li_2MnO_3.

RESULTS AND DISCUSSION

This investigation is used for finding the best cathode material compositions including $(1 - n - m)LiCo_{0.8}Ni_{0.2}O_2$, nLi_2MnO_3, $mLiNiO_2$ systems with high initial discharge capacity, good cyclability and inexpensive cost compared to current lithium-ion cathode materials. Therefore, initially, 28 different composition points according to using the lever rule, stoichiometric weights and mole-fractions were chosen in order to find an optimized material with good electrochemical performance. These 28 points were extracted through the triangle phase diagram of the defined system (Scheme 1 and Tables 2 and 3) and were synthesized through the sol–gel methods. Scanning electron micrographs were performed to characterize the approximate size and surface morphologies of the various composition and as shown in Schemes 3 and 4, the $LiCo_{0.8}Ni_{0.2}O_2$ and Li_2MnO_3 materials appear to be homogeneous size distribution with submicron particle sizes. In fact, those particles of these materials synthesized via sol–gel methods might be favorable for the intercalation and de-intercalation mechanism of electrodes during the charge–discharge processes which are suitable for delivering large and larger amount of capacities. Similar size distributions and morphologies are observed for Mn doped materials in various mole fraction which suggests that the Mn is well permeated into the bare $LiCo_{0.8}Ni_{0.2}O_2$ for producing the ideal composition of $Li_{1.333}Ni_{0.4}Co_{0.267}Mn_{0.333}O_2$ for forming a solid solution (Scheme 5) which indicates that Mn ions are homogeneously dissolved into the colloidal precursor in the solution prior to following heat treatments for calcination.

Besides, these kind particle sizes of $Li_{1.333}Ni_{0.4}Co_{0.267}Mn_{0.333}O_2$ desire for improving the electrochemical efficiency of the electrodes through reducing the ion diffusion during ion lithium intercalation and de-intercalation mechanism. The electrochemical efficiencies of these systems have been evaluated at room and also high temperatures, therefore, the charge–discharge curves appear to be quite monotonous and no major structural transitions occur during the lithium extraction/insertion reactions.

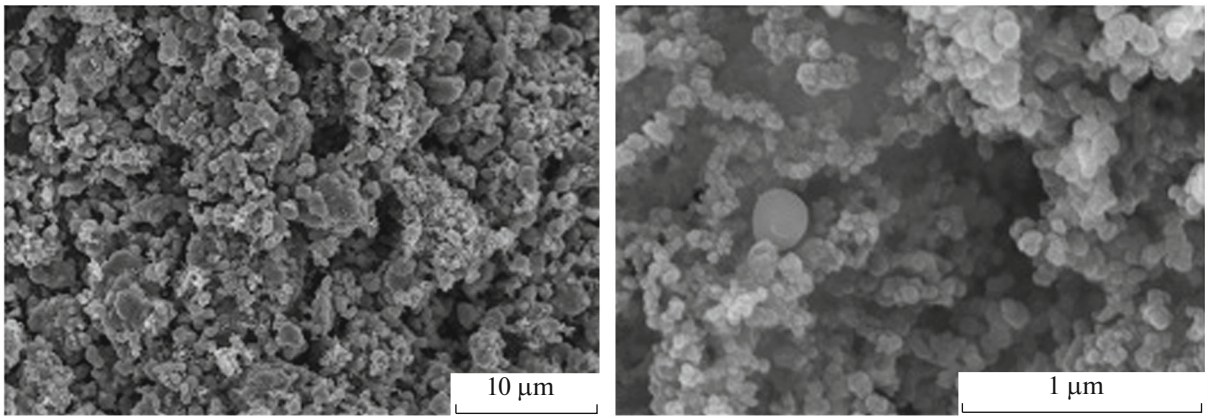

Scheme 5. Scanning electron micrograph obtained for $Li_{1.333}Ni_{0.4}Co_{0.267}Mn_{0.333}O_2$.

As it can be seen in Table 2 and Scheme 1, cobalt decreases towards down direction of triangle, meanwhile the compositions of 22 has zero Ni percentage. High Mn value is found at sample 22 and its content decreases at the opposite end points of the triangle. Nickel percentage is found in a wide region in the triangle and also

Table 3. Summary capacity and cyclability for 28 samples of the system $(1 - n - m)LiCo_{0.8}Ni_{0.2}O_2$

Sample	Blend	Li_2MnO_3	$LiNiO_2$	$(1 - n - m)$ $LiCo_{0.8}Ni_{0.2}O_2$	Capacity, mA h g^{-1}	Cyclability
1	Pure	0	0	1	172.5	49
2	Binary	0.167	0	0.833	112.3	47
3	Binary	0	0.167	0.833	109.5	48
4	Binary	0.333	0	0.667	125.5	51
5	Ternary	0.167	0.167	0.667	149.5	58
6	Binary	0	0.333	0.667	79.5	69
7	Binary	0.500	0	0.500	173.5	71
8	Ternary	0.333	0.167	0.500	155.2	51
9	Ternary	0.167	0.333	0.500	159.8	71
10	Binary	0	0.500	0.500	149.5	70
11	Binary	0.667	0	0.333	258.5	69
12	Ternary	0.500	0.167	0.333	256.5	97
13	Ternary	0.333	0.333	0.333	255.5	99
14	Ternary	0.167	0.500	0.333	253.5	89
15	Binary	0	0.667	0.333	140.6	99
16	Binary	0.833	0	0.167	171.5	70
17	Ternary	0.667	0.167	0.167	151.5	98
18	Ternary	0.500	0.333	0.167	210.2	99
19	Ternary	0.333	0.5	0.167	247.5	99
20	Ternary	0.167	0.667	0.167	201.5	50
21	Binary	0	0.833	0.167	179.5	95
22	Pure	1	0	0	140.5	90
23	Binary	0.833	0.167	0	199.5	95
24	Binary	0.667	0.333	0	255.5	94
25	Binary	0.500	0.500	0	249.5	99
26	Binary	0.333	0.667	0	175.5	45
27	Binary	0.167	0.833	0	155.5	74
28	Pure	0	1	0	223.2	90

decreases near Li_2MnO_3 or $Li(Li_{0.33}Mn_{0.66})O_2$. It is predicted which capacities and cyclability of the compositions are directly related to the amount of Mn, Co, and Ni. It is notable, specific capacity is determined as the charge which can be reserve in volume or mass (A h), while the rate capability (which are related to their design and varies considerably between different manufactures), can be determined as the rate at which the cell is being charged. Therefore the C-rate is the capacity of the battery divided by the hourly charging rate. The discharge capacity curves of this work have been compared with 18650-type "$C/LiCoO_2$ Sony battery" result which is modified by Ehrlich [26].

Since $LiCoO_2$ cathode has an initial discharge capacity around 145 mA h/g [27], therefore any materials of these compositions with initial capacities more than this amount (of course with a suitable cyclability) might be considered. The samples were tested via a cycler (Arbin BT 2000 battery testing system), between 2.4 and 4.6 V with low C-rate of C/10. The initial results indicate of a wide range and irregular of cyclability and capacities. The initial discharge capacities varied from 172.5 to 258.5 mA h/g. Both capacity and cyclability increase from $LiCo_{0.8}Ni_{0.2}O_2$ towards the binary composition of Li_2MnO_3 and $LiNiO_2$.

In this work the SATISTICA software has been used for analyzing the data which Var1, Var2, Var3, are Li_2MnO_3, Li_2NiO_2 and $(1 - n - m)LiCo_{0.8}Ni_{0.2}O_2$ respectively while the Var4 alternately, are the capacity and cyclability (Table 3 and Figs. 1–3).

Figure 2 presents the voltage versus capacity profiles of some samples for $(1 - n - m)LiCo_{0.8}Ni_{0.2}O_2$, mLi_2MnO_3 and $nLiNiO_2$ compositions of cathode materials in the initial charges/discharges cycles. Although sample (11) shows high capacity (around 258.5 mA h g^{-1}), it contains of a low cyclability. The samples 13, 25 and 19 exhibit good capacity of 255.5, 249.5, and 247.5 mA h/g, respectively with high cyclability, meanwhile due to Mn^{4+} ion the sample 22 has a low capacity. Although these kinds of data are not sufficient for determining a suitable cathode material in view point of capacity and cyclability amount, the statistical analysis can be useful for finding the region of the best item from the data of the 28 compositions. Therefore any testing with both capacity and cyclability relation in view point of the triangle regions is needed.

By this work various compositions are used for exploring the novel cathode materials with two-dimensional layered structure through the ternary composition's diagram among iso-structural material.

Although Li_2MnO_3 or $Li(Li_{1/3}Mn_{2/3})O_2$ has a structure similar to $LiCoO_2$, there is super-lattice ordering of Mn^{4+} and Li^+ in transition layers. $(1 - n - m)LiCo_{0.8}Ni_{0.2}O_2$ can be demonstrated as solid solution between $LiCoO_2$ and $LiNiO_2$, is a promising cathode material because of its improved stabilities and electrochemical performances.

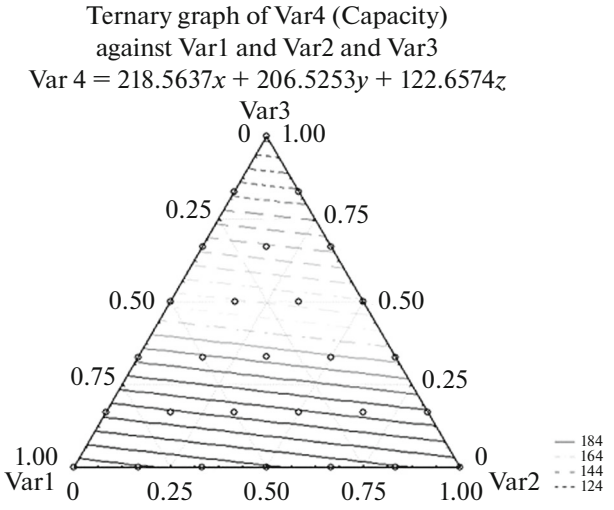

Fig. 1. Ternary of capacity versus Var1, Var2 and Var3 for 28 samples of Li_2MnO_3, Li_2NiO_2 and $(1 - n - m)LiCo_{0.8}Ni_{0.2}O_2$ respectively.

Through an analyzing among these compositions, three samples were chosen and subsequently synthesized, characterized and tested consequently with high precision. Via initial discharge capacity and some extra results nos. 11, 12, 13 and 14 (Figs. 4 and 5, Tables 2 and 3). As the number 11 is binary cannot be consider for a suitable cathode material candidate. As it can be seen in Fig. 6 between two numbers of 0.1 and 0.22 in the X axis, an overlapping range between capacity and cyclability can be observed for $(1 - n - m)LiCo_{0.8}Ni_{0.2}O_2$.

Meanwhile based on Fig. 7, nos. 13 and 14 are completely located on the red and blue lines and based Fig. 8 no. 13 ($Li_{1.333}Ni_{0.4}Co_{0.267}Mn_{0.333}O_2$) has the most efficiency between 28 cathode materials for lithium ion battery and is suggested as the best composition for cathode material by this work. Obviously, the used weight of cobalt in these samples is lower compared with $LiCoO_2$ that is an advantage in view point of cost and toxic in this study.

Charge–discharge characteristics of $Li_{1.333}Ni_{0.4}Co_{0.267}Mn_{0.333}O_2$ were investigated by performing cycle tests in the range of 2.4–4.6 V. The increase in specific capacity for $Li_{1.333}Ni_{0.4}Co_{0.267}Mn_{0.333}O_2$ could be attributed to the enhancement of layered characteristics with Mn. The repeat of sample 13 was made into T-Cells and subjected to electrochemical testing using the original conditions and the cycling was accomplished between 2.4–4.6 V with constant C-rate of C/10 at room temperature (Fig. 9). The repeat sam-

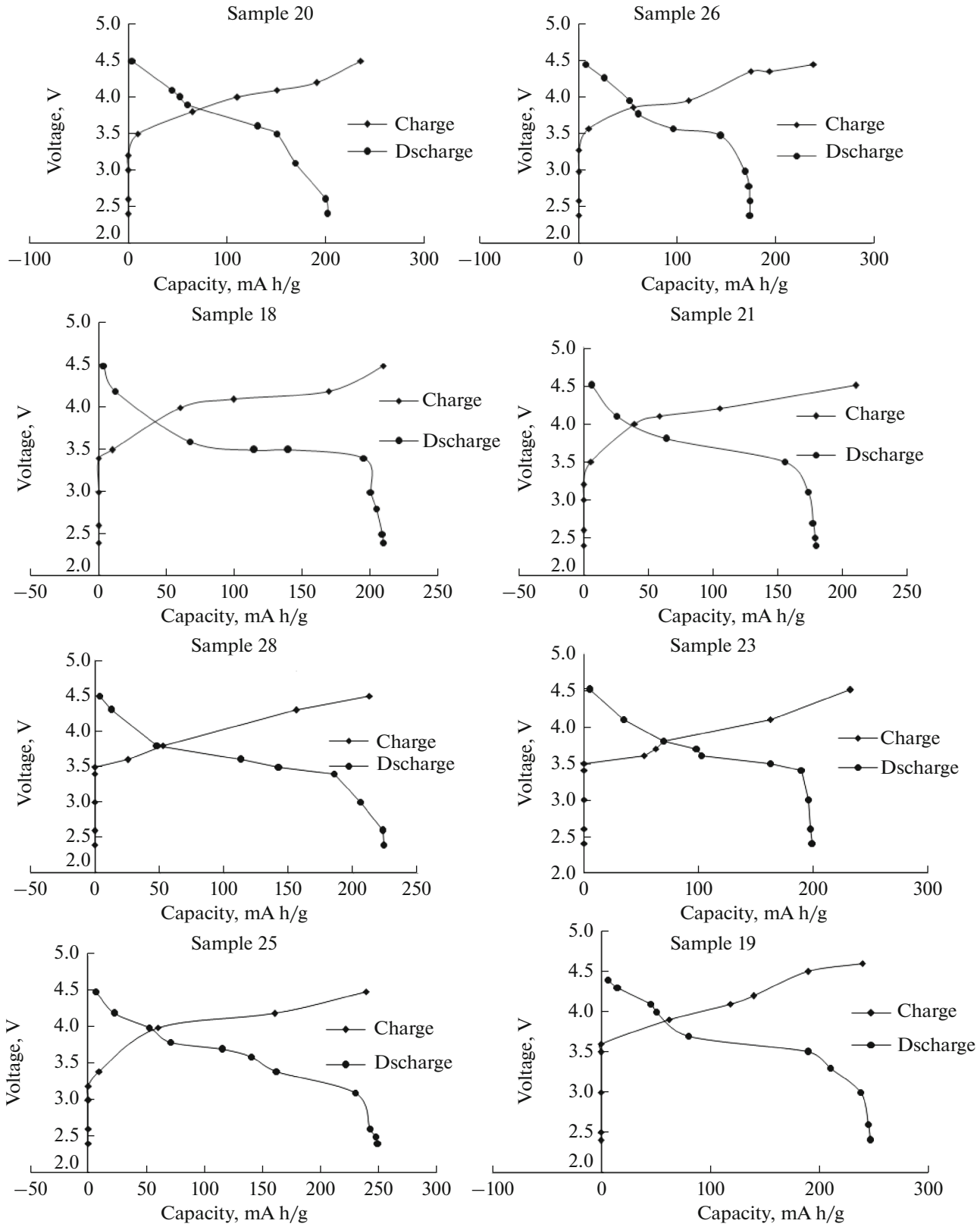

Fig. 2. Charge and discharge diagrams of various samples.

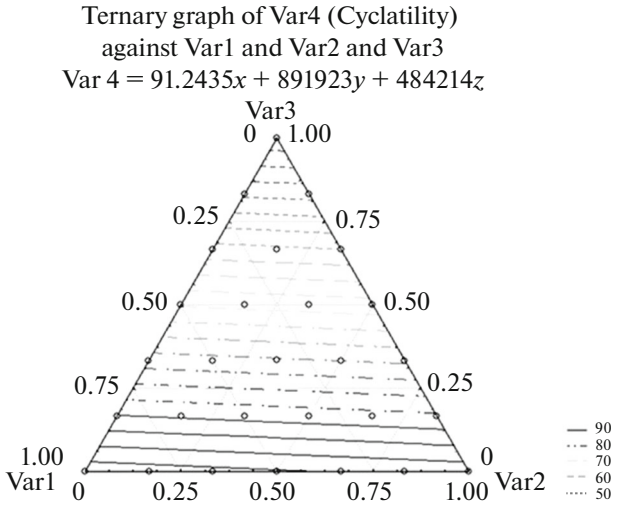

Fig. 3. Ternary of cyclability versus Var1, Var2 and Var3 for 28 samples of Li_2MnO_3, Li_2NiO_2 and $(1 - n - m)LiCo_{0.8}Ni_{0.2}O_2$ respectively.

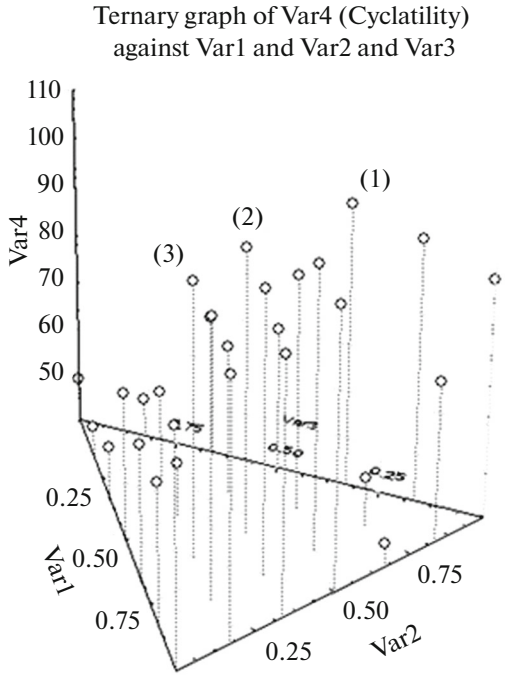

Fig. 5. Three samples of $(1 - n - m)LiCo_{0.8}Ni_{0.2}O_2$ (Var3), mLi_2MnO_3 (Var1), $nLiNiO_2$ (Var2) composites with high precisionist of cycalability versus Var1, Var2 and Var3.

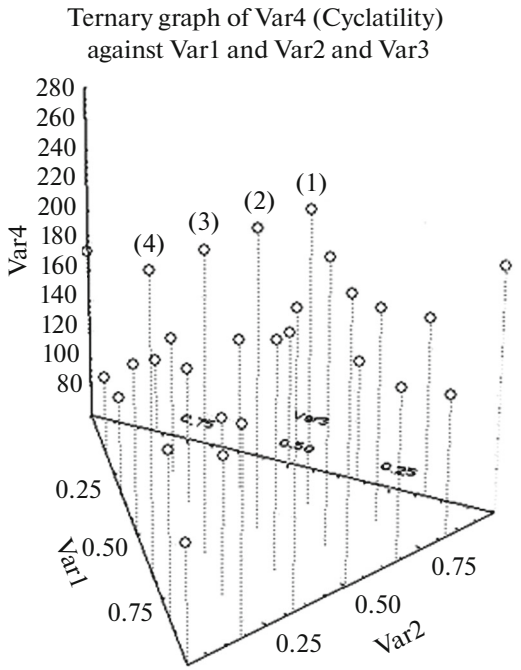

Fig. 4. Three samples of $(1 - n - m)LiCo_{0.8}Ni_{0.2}O_2$ (Var3), mLi_2MnO_3 (Var1), $nLiNiO_2$ (Var2) composites with high precisionist of capacity versus Var1, Var2 and Var3.

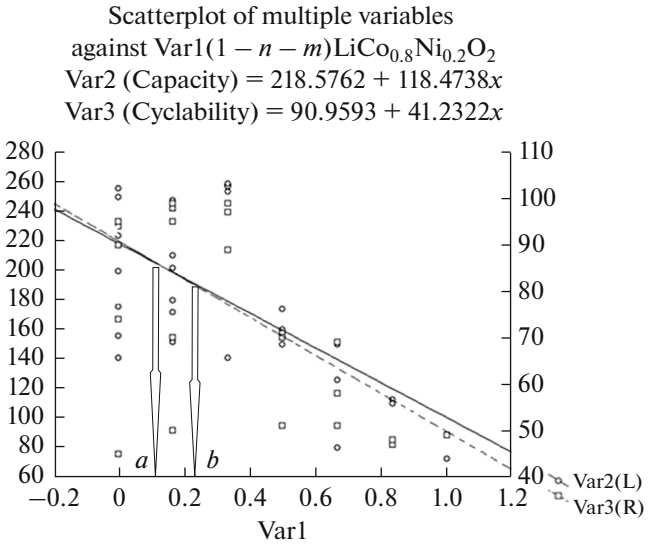

Fig. 6. The regions between *a* and *b* has an overlapping between capacity and cyclability lines.

ple exhibits better charge and discharge capacities than the original sample. This improvement in the capacities is attributed to the synthesis conditions.

CONCLUSIONS

$(1 - n - m)LiCo_{0.8}Ni_{0.2}O_2$, mLi_2MnO_3, $nLiNiO_2$ composition of cathodes with submicron particles have been successfully synthesized by a sol–gel

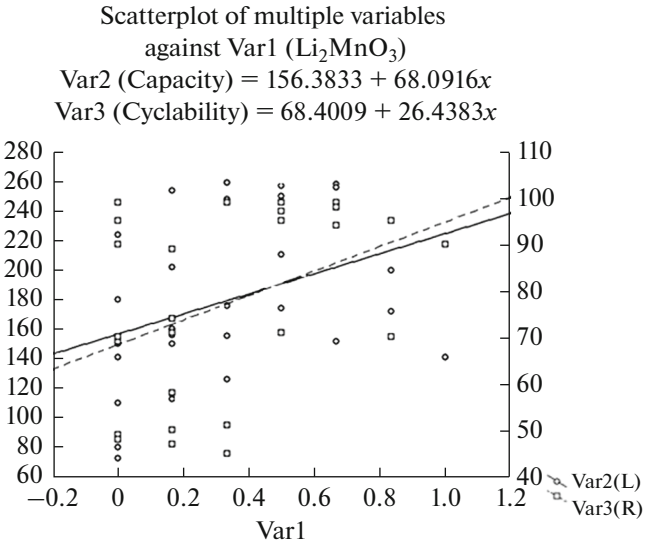

Fig. 7. Capacity and cyclability lines versus Li_2MnO_3.

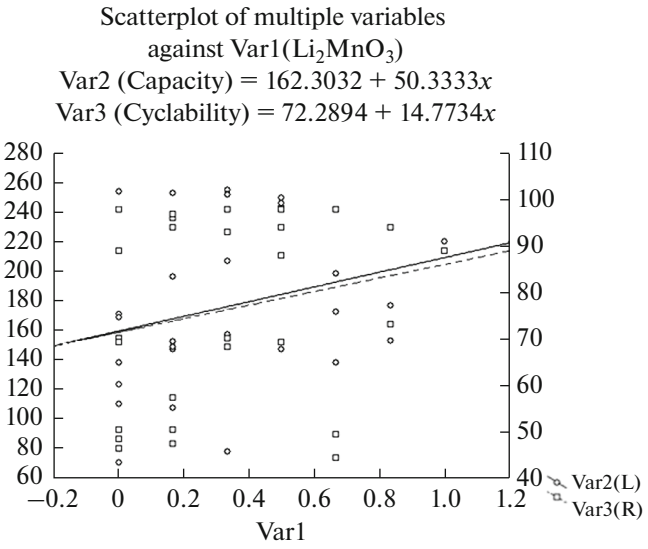

Fig. 8. Capacity and cyclability lines versus Li_2NiO_2.

method. The structural and electrochemical properties have been systemically investigated to examine the effects of charge/discharge capacities and also capacity retention. The results show that all the prepared "$Li_{1.1333}Ni_{0.4}Co_{0.267}Mn_{0.333}O_2$" type layered structure regardless of the nickel content improve the capacity retention significantly. Moreover, suppresses the phase transitions that usually occur in $LiNiO_2$ during cycling and improves the charge–discharge reversibility of composition with $Li_{1.1333}Ni_{0.4}Co_{0.267}Mn_{0.333}O_2$ structure. The percentage of nickel and cobalt exhibit a good performance. Although these kind systems can help for removing the disadvantage of cobalt which

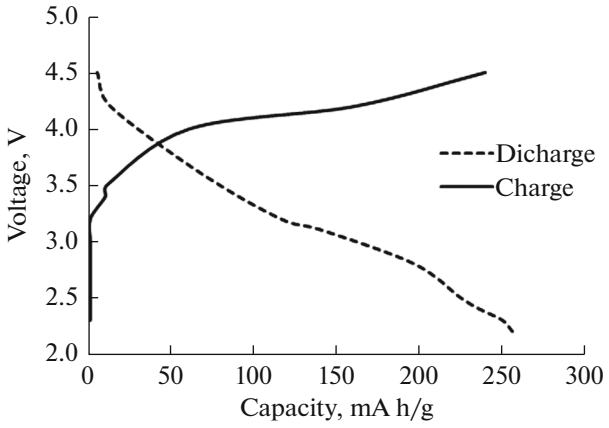

Fig. 9. Charge and discharge capacity of $Li_{1.333}Ni_{0.4}Co_{0.267}Mn_{0.333}O_2$.

mainly is its cost and toxic, the performance of these kind systems is similar to $LiCoO_2$ cathode material. Therefore fabrication of lithium-ion batteries using a few more transition elements such as Mn, Al and Mg is suggested for any further research.

FUNDING

This research is funded by Vietnam National University—Ho Chi Minh city (VNU-HCM) under the grand no. TX2019-32-01.

CONFLICT OF INTEREST

The authors declare that they have no conflict of interest.

REFERENCES

1. *Advances in Lithium-Ion Batteries,* Nishi, Y., Van Schalkwijk, W.A., and Scrosati, B., Eds., Boston, MA: Kluwer/Springer, 2002.
2. *Lithium-Ion Batteries, Science and Technologies,* Yoshio, M., Brodd, R.J., and Kozawa, A., Eds., New York: Springer-Verlag, 2009.
3. Scrosati, B. and Garche, J., Lithium batteries: status, prospects and future, *J. Power Sources,* 2010, vol. 195, no. 9, p. 2419.
4. Daniel, C. and Besenhard, J.O., *Handbook of Battery Materials,* 2nd ed., Wiley-VCH, 2011.
5. Meyers, R.A., *Encyclopedia of Sustainability Science and Technology,* New York: Springer, 2012.
6. Rossen, E., Jones, C.D.W., and Dahn, J.R., Structure and electrochemistry of $Li_xMn_yNi_{1-y}O_2$, *Solid State Ionics*, 1992, vol. 57, no. 3-4, p. 311.
7. Spahr, M.E., et al., Characterization of layered lithium nickel manganese oxides synthesizedbya novel oxidative co-precipitation method and their electrochemical performance as lithium insertion electrode materials, *J. Electron. Soc.,* 1998, vol. 145, no. 4, p. 1113.
8. Ohzuku, T. and Makimura, Y., Layered lithium insertion material of $LiNi_{1/2}Mn_{1/2}O_2$: a possible alternative

to $LiCoO_2$ for advanced lithium-ion batteries, *Chem. Lett.*, 2001, vol. 30, no. 8, p. 744.

9. Makimura, Y. and Ohzuku, T., Lithium insertion material of $LiNi_{1/2}Mn_{1/2}O_2$ for advanced lithium-ion batteries, *J. Power Sources*, 2003, vols. 119–121, p. 156.
10. Liu, Z., Yu, A., and Lee, J.Y., Synthesis and characterization of $LiNi_{1-x-y}Co_xMn_yO_2$ as the cathodematerials of secondary lithium batteries, *J. Power Sources*, 1999, vol. 81–82, p. 416.
11. Yoshio, M., et al., Preparation and properties of $LiCo_yMn_xNi_{1-x-y}O_2$ as a cathode for lithium ion batteries, *J. Power Sources*, 2000, vol. 90, no. 2, p. 176.
12. Ohzuku, T. and Makimura, Y., Layered lithium insertion material of $LiCo_{1/3}Ni_{1/3}Mn_{1/3}O_2$ for lithium-ion batteries, *Chem. Lett.*, 2001, vol. 30, no. 7, p. 642.
13. Belharouak, I., et al., $Li(Ni_{1/3}Co_{1/3}Mn_{1/3})O_2$ as a suitable cathode for high power applications, *J. Power Sources,* 2003, vol. 123, no. 2, p. 247.
14. Ngala, J.K., et al., The synthesis, characterization and electrochemical behavior of the layered $LiNi_{0.4}Mn_{0.4}Co_{0.2}O_2$ compound, *J. Mat. Chem.*, 2004, vol. 14, no. 2, pp. 214–220.
15. Yoon, W.S., et al., A comparative study on structural changes of $LiCo_{1/3}Ni_{1/3}Mn_{1/3}O_2$ and $LiNi_{0.8}Co_{0.15}Al_{0.05}O_2$ during first charge using in situ XRD, *Electrochem. Commun.,* 2006, vol. 8, no. 8, p. 1257.
16. Ammundsen, B., et al., Local structure and first cycle redox mechanism of layered $Li_{1.2}Cr_{0.4}Mn_{0.4}O_2$ cathode material, *J. Electron. Soc.*, 2002, vol. 149, no. 4, p. A431.
17. Thackeray, M.M., et al., Advances in manganese-oxide composite electrodes for lithium-ion batteries, *J. Mat. Chem.,* 2005, vol. 15, no. 23, p. 2257.
18. Zhang, L., Noguchi, H., and Yoshio, M., Synthesis and electrochemical properties of layered Li–Ni–Mn–O compounds, *J. Power Sources,* 2002, vol. 110, no. 1, p. 57.
19. Shin, S.S., Sun, Y.K., and Amine, K., Synthesis and electrochemical properties of $Li[Li_{(1-2x)/3}Ni_xMn_{(2-x)/3}]O_2$ as cathode materials for lithium secondary batteries, *J. Power Sources,* 2002, vol. 112, no. 2, p. 634.
20. Hailang, Z. and Wen-Hua, S., Synthesis and characterization of $LiNi_{0.7-x}Mg_xCo_{0.3}O_2$ ($0 \le x \le 0.1$) cathode materials for lithium-ion batteriesprepared by a sol–gel method, *Adv. Mater. Sci. Eng.*, 2014, no. 3, p. 1.
21. Monajjemi, M., Mahdavian, L., and Mollaamin, F., Characterization of nanocrystalline silicon germanium film and nanotube in adsorption gas by Monte Carlo and Langevin dynamic simulation, *Bull. Chem. Soc. Ethiopia,* 2008, vol. 22, no. 2, p. 277.
22. Lee, V.S., Nimmanpipug, P., Mollaamin, F., Thanasanvorakun, S., and Monajjemi, M., Investigation of single wall carbon nanotubes electrical properties and normal mode analysis: dielectric effects, *Russ. J. Phys. Chem. A,* 2009, vol. 83, no. 13, p. 2288.
23. Monajjemi, M. and Ahmadianarog, M., Carbon nanotube as a deliver for sulforaphane in Broccoli vegetable in point of nuclear magnetic resonance and natural bond orbital specifications, *J. Comput. Theor. Nanosci.,* 2014, vol. 11, no. 6, p. 1465.
24. Monajjemi, M., Farahani, N., and Mollaamin, F., Thermodynamic study of solvent effects on nanostructures: phosphatidylserine and phosphatidylinositol membranes, *Phys. Chem. Liq.,* 2012, vol. 50, no. 2, p. 161.
25. Monajjemi, M., Mahdavian, L., Mollaamin, F., and Honarparvar, B., Thermodynamic investigation of enolketotautomerism for alcohol sensors based on carbon nanotubes as chemical sensors, *Fullerenes, Nanotubes, Carbon Nanostruct.,* 2010, vol. 18, no. 1, p. 45.
26. Ehrlich, G.M. and Linden, D., *Handbook of Lithium-Ion Batteries,* McGraw-Hill, 2002, p. 35.
27. Yang, Z., Zhang, J., Kintner-Meyer, M.C.W., Lu, X., Choi, D., Lemmon, J.P., and Liu, J., Electrochemical energy storage for green grid, *Chem. Rev.,* 2011, vol. 111, p. 3577.